Supplemental data

Supplemental methods

EAE mice model. EAE was induced by complete Freund's adjuvant (CFA)-MOG35-55 peptide immunization (China Peptides Biotechnology) and scored daily. Briefly, C57BL/6J mice were injected subcutaneously into the base of the tail and both flanks with a volume of 200 μl containing 200 μg MOG35-55 peptide emulsified in complete Freund's adjuvant (Sigma-Aldrich). Mice were also injected intraperitoneally with 500 ng of pertussis toxin (Sigma-Aldrich) on days 0 and 2 postimmunization. All reagents used for the in vivo experiments were free of endotoxin. Mice were monitored daily for the development of disease, which was scored according to the following scale: 0, no symptoms; 1, tail weakness; 2, tail paralysis and hind limb weakness; 3, complete hind limb paralysis; 4, hind limb paralysis with forelimb weakness and 5, moribund or death.

Generation of bone marrow chimeric mice. One week before irradiation, feed the recipient mice with medicated water. Bone marrow cells were prepared from WT or miR-210 KO donor mice and adoptively transferred into lethally irradiated (950 rad, in two divided doses) miR-210 KO or WT recipient mice (8-week-old, 1×10^7 per mouse). After transplantation, the recipient mice were continue to give medicated water for one week. After 8 weeks, the chimeric mice were subjected for psoriasis-like mouse model induction.

Adoptive transfer of naïve $CD4^+$ T cells. Spleens from donor WT and miR-210 KO mice were homogenized in complete RPMI 1640 medium (Gibco, USA) and passed through a 40 μm cell strainer to yield a single cell suspension. Naïve $CD4^+$ T cells were isolated by negative selection using the mouse naïve $CD4^+$ T cell isolation

kit II (Miltenyi Biotech) according to the manufacturer's instruction. *Rag2*$^{-/-}$ recipient mice were administered with 5×10^6 cells from WT or miR-210 KO mice spleen (suspended in 200 μl sterile PBS) via tail vein injection. Control *Rag2*$^{-/-}$ mice were injected with 200 μl PBS. After one week, the reconstituted mice were subjected for psoriasis-like mouse model induction.

Immunofluorescence staining. Six-micron-thick frozen sections of IMQ-induced mouse psoriasis-like specimens and control specimens from healthy mice were used for immunofluorescence analysis. After the sections were fixed for 15 min at RT in 4% paraformaldehyde, they were washed three times in PBS and incubated in Blocking Buffer (1% BSA in 1× PBS) for 1 h. Anti-mouse CD4-FITC Ab (BioLegend, USA, Cat: 100406) was diluted 1:50 in Blocking Buffer. Sections were stained with anti-CD4 rabbit Ab and incubated overnight at 4℃. After being washed in PBS and air-dried, sections were stained with DAPI (Invitrogen, USA). Image analysis was performed using the fluorescence microscope DMI 4000B (Leica, Germany) and Leica Qwin Std analysis software.

Keratinocyte culture. Normal human epidermal keratinocytes (NHEK, PromoCell, Germany, Cat: C-12006) stored in liquid nitrogen were defrosted and cultured in serum-free basal medium with supplementMix (PromoCell, Germany). HaCaT cells stored in liquid nitrogen were revived and cultured in DMEM (Gibco, USA) with 10% FBS (Gibco, USA) at 37℃, 5% CO_2. Medium was refreshed every 2 days and cells were subcultured according to the cell fusion. Cells at passage 2-6 were used for subsequent experiments.

*Cytokines stimulation of keratinocytes***.** NHEK or HaCaT cells were stimulated with TGF-β (5 ng/ml, PeproTech), IL-23 (20 ng/ml, PeproTech), IL-6 (10 ng/ml, PeproTech), IL-1β (10 ng/ml, PeproTech), IL-17A (200 ng/ml, PeproTech) and IFN-

γ (200 ng/ml, PeproTech), respectively. The cells and culture supernatant were collected at corresponding time point for the subsequent experiments.

Transfection of keratinocytes. NHEK were seeded in 24-well plate with 1 ml serum-free basal medium one day before transfection. Then 2 μl 200 μM agomir-210/antagomir-210 or their corresponding controls were added into the medium for the purpose of transfection. After 6 h, the medium was removed and new 1 ml serum-free basal medium with supplementMix and 1 μl 200μM agomir-210/antagomir-210 or their corresponding controls were added into the well for another 48h. Then, the cells and culture supernatant were collected for the subsequent experiments.

CCK8 assay. NHEK were seeded in 96-well plates in triplicates followed by transfection with agomir-210 or antagomir-210, then cells were cultured in 100 μl serum-free basal medium with supplementMix for 24 h or 48 h. The Cell Counting Kit-8 (CCK8, Beyotime, China) was used to evaluate cell proliferation. Briefly, 10 μl CCK8 solution was added to each well, and cells were incubated for 3 h at 37℃, 5% CO_2. Cell viability was detected at 450 nm.

Enzyme linked immunosorbent assay (ELISA). The level of TGF-β and CCL20 in the culture supernatant of keratinocytes were detected using the Human TGF-β ELISA Kit and Human CCL20 ELISA Kit (4A Biotech Co., Beijing, China) according to manufacturer's instructions. Briefly, serially diluted standards and samples (1:2 dilution) were added into the wells (100 μl/well) and incubated at 37℃ for 90 min. Plate were washed four times with the washing buffer. Biotinylated antibody working solution (100 μl/well) were added to the wells, which were incubated at 37℃ for 1 h followed by washing four times. HRP-conjugated avidin at a dilution of 1:100 (100 μl/well) were added to the cells, and were incubated at 37℃ for 30 min. Then the plate was washed four times and incubated with DAB solution

(100 μl/well) for 10-20 min at 37℃. Reactions were terminated with stopping solution (100 μl/well) and OD450 values were obtained. Concentration of the cytokines were extrapolated from the standard curve.

Cell chemotaxis assay. Transwell assays (pore size 5.0 μm, Corning, USA) were performed to assess the chemotaxis of keratinocytes transfected with agomir-210/antagomir-210 or stimulated with TGF-β to $CD4^+$ T cells. $CD4^+$ T cells (5×10^5) were suspended in 200 μl serum-free RPMI 1640 (Gibco, USA) medium, and were seeded into the upper chambers in triplicates. 600 μl culture supernatant collected from NHEK transfected with agomir-210/antagomir-210 or stimulated with TGF-β was added to the lower chambers respectively as a chemotactic factor. Following a 90 min incubation in 37℃, 5% CO_2, the non-migrated cells on the upper surface of the filter were carefully removed with a cotton swab. Cells that migrated through the 5.0 μm sized pores and adhered to the lower surface of the filter were fixed with 90% ethanol for 15 min and then were stained with 0.1% crystal violet followed by washing with deionized water. Cells in five non-overlapped fields were counted under a microscope DMI 4000B (Leica, Germany), and the mean cell counts were calculated.

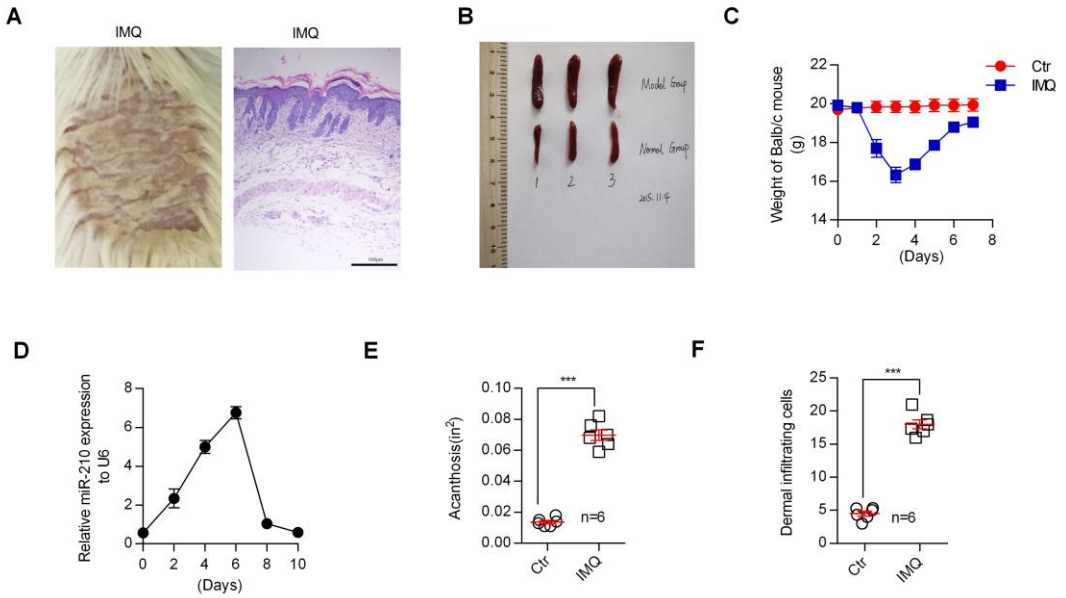

Supplemental Figure 1. IMQ-induced psoriasis-like mouse model. IMQ cream was painted on the shaved back skin of BALB/c mice for 7 consecutive days. (**A**) Phenotypic presentation and H&E staining of lesional skin from IMQ-treated mice. Scale bar: 100μm. (**B**) Splenomegaly of mice treated with IMQ. (**C**) Mouse weight was measured during IMQ application (Ctr, n=6; IMQ, n=6). (**D**) miR-210 expression during the establishment of the psoriasis-like model was determined by RT-qPCR (n=6). (**E** and **F**) Acanthosis and dermal cellular infiltrates were quantitated for untreated mice (n=6) and IMQ-treated mice (n=6). All data are representative of at least three independent experiments with three to six samples per group in each. Data represent the mean ± SEM. ***$P < 0.001$. Two-tailed unpaired Student's *t*-test (**E** and **F**) was used. Ctr, untreated mice; IMQ, IMQ-treated mice.

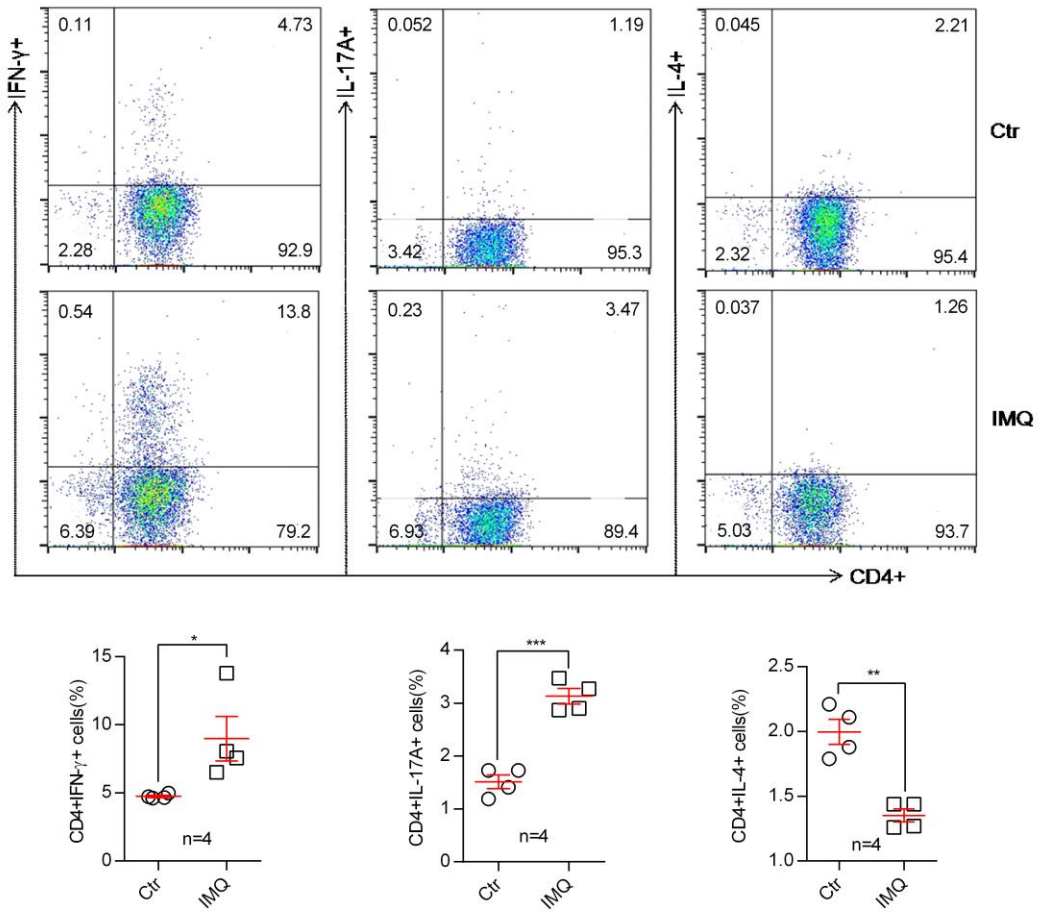

Supplemental Figure 2. T_H cell-mediated immune imbalance in the IMQ-induced psoriasis-like mouse model. The percentage of T_H1, T_H2 and T_H17 cells in splenic $CD4^+$ T cells of IMQ-treated (n=4) or untreated BALB/c mice (n=4) in Supplemental Figure 1 was detected by flow cytometry (upper panel). The statistical data are shown in the lower panel. All flow cytometry figures represent one set of experiments with four samples per group. Data represent the mean ± SEM. **P* < 0.05, ***P* < 0.01, ****P* < 0.001. Two-tailed unpaired Student's *t*-test was used. Ctr, untreated mice; IMQ, IMQ-treated mice.

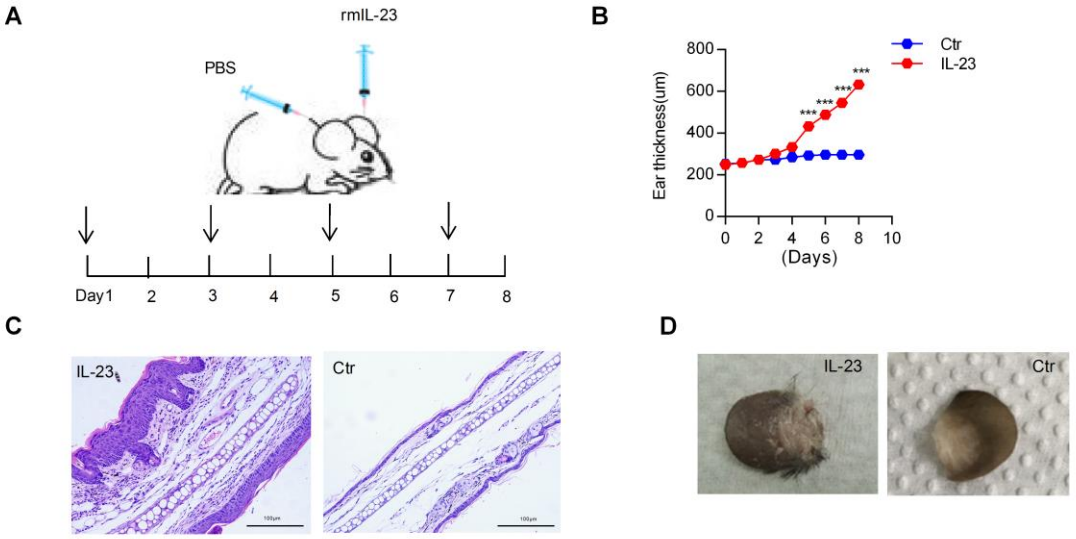

Supplemental Figure 3. IL-23-induced psoriasis-like mouse model. (**A**) Schematic diagram for intradermal administration of IL-23. Ears of C57BL/6J mice were injected intradermally with 1 mg rmIL-23 dissolved in 25 µl PBS into one ear and 25 µl PBS into the contralateral ear. Injections were continued every other day for 8 days (days 1, 3, 5 and 7). (**B**) Ear thickness was measured on the indicated days (n=5). (**C** and **D**) H&E staining (**C**) and phenotypic presentation (**D**) of ears injected with PBS and ears injected with IL-23. Scale bar: 100µm. Data are representative of at least three independent experiments with five samples per group in each. Data represent the mean ± SEM. ***P < 0.001.Two-tailed unpaired Student's t-test (**B**) was used. Ctr, PBS-treated ears.

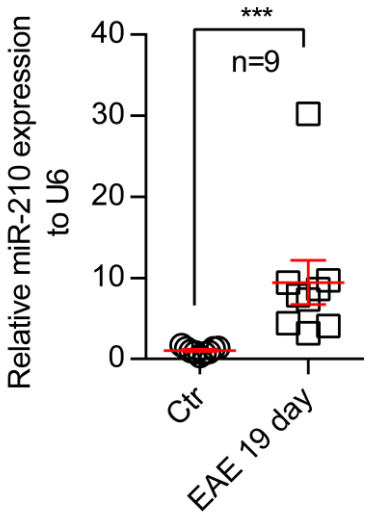

Supplemental Figure 4. miR-210 expression is increased in EAE mice model. The expression of miR-210 in splenic $CD4^+$ T cells from the EAE mice (19^{th} day, n=9) and control mice (n=9) was detected. The EAE model was induced in C57BL/6J mice. Data represent the mean ± SEM. ***$P < 0.001$. Two-tailed Mann-Whitney *U*-test was used.

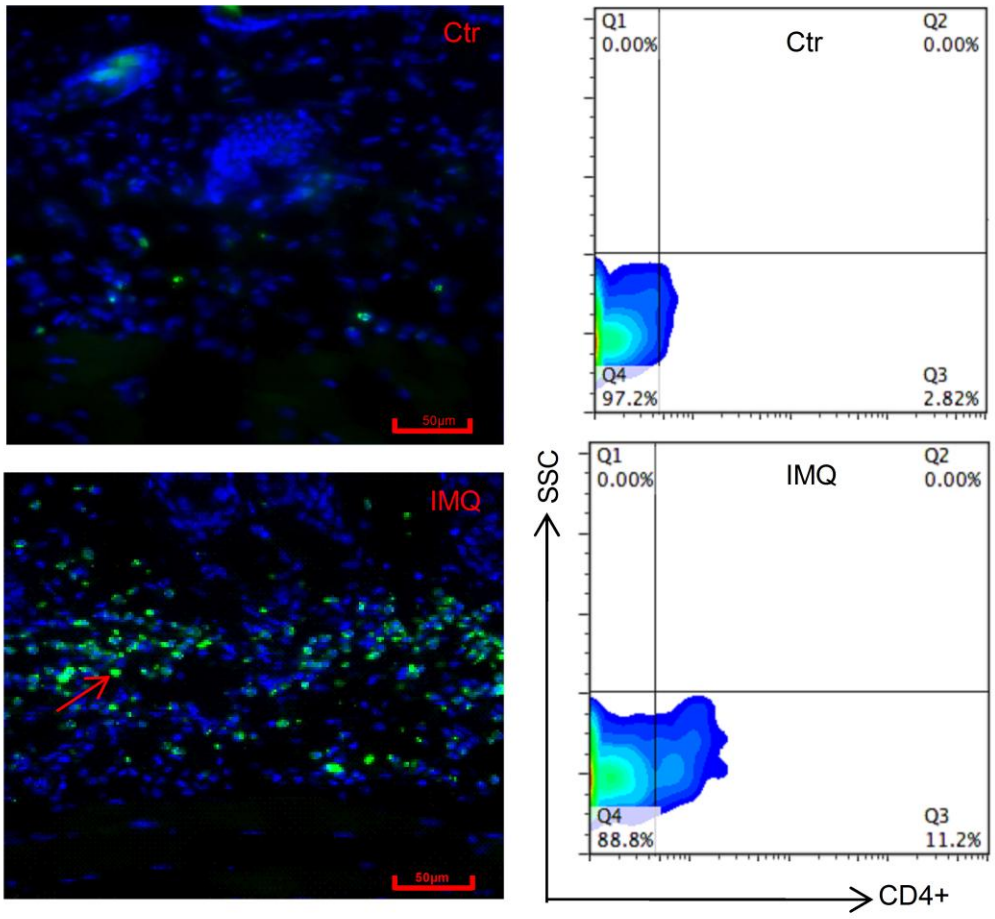

Supplemental Figure 5. CD4$^+$ T cells are increased in the psoriatic dermis. Immunofluorescence was performed on mouse skin from untreated BALB/c mice (Ctr) and IMQ-treated BALB/c mice (IMQ) to detect dermal CD4$^+$ T cells (left panel). Scale bar, 50 μm; red arrows indicate dermal CD4$^+$ T cells. Then, dermal single-cell suspension was obtained from healthy skin of Ctr and lesional skins of IMQ, and the proportion of CD4$^+$ T cells was detected by flow cytometry (right panel). The experiment was repeated at least three times.

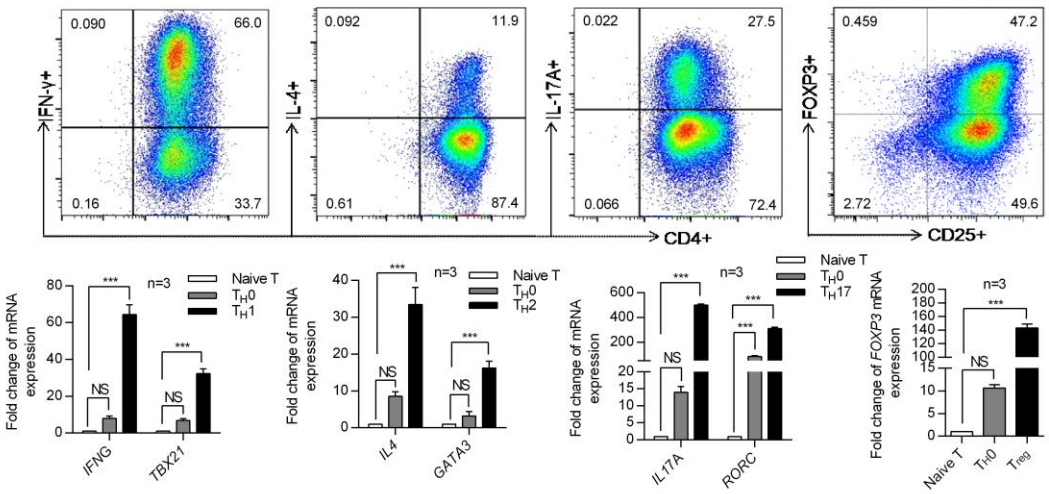

Supplemental Figure 6. In vitro differentiation of human naïve CD4$^+$ T cells. Naïve CD4$^+$ T cells from human peripheral blood were stimulated with plate-bound anti-CD3 and soluble anti-CD28 under T_H0-, T_H1-, T_H2-, T_H17- and T_{reg}-polarizing conditions in vitro. Five days later, the percentages of T_H1, T_H2, T_H17 and iT_{reg} cells was detected by flow cytometry (upper panel). The mRNA levels of corresponding specific cytokines and transcription factors in naïve CD4$^+$ T cells, T_H0 cells and polarized T_H cells were detected by RT-qPCR (n=3). All flow cytometry figures represent one set of experiments, and each experiment was repeated at least three times on different individuals. Data represent the mean ± SEM. ***P < 0.001, NS: not significant. One-way ANOVA with Dunnett *post hoc* test was used.

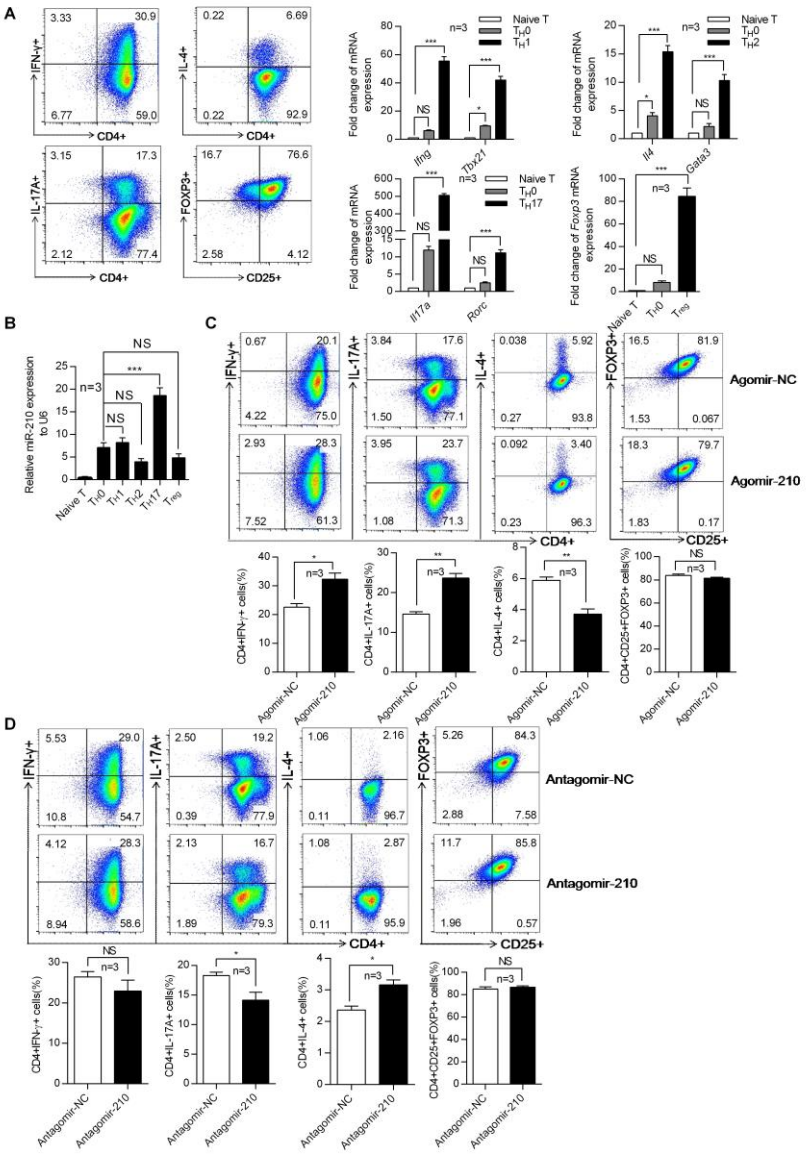

Supplemental Figure 7. miR-210 regulates T cells differentiation in mice. (**A** and **B**) Naïve $CD4^+$ T cells from mouse spleen were stimulated with plate-bound anti-CD3 and soluble anti-CD28 under T_H0-, T_H1-, T_H2-, T_H17- and T_{reg}-polarizing conditions in vitro (n=3). Five days later, the percentages of T_H1, T_H2, T_H17 and iT_{reg} cells was detected by flow cytometry (**A**, four panels on the left). The mRNA expression of corresponding specific cytokines and transcription factors (**A**, four panels on the right), as well as miR-210 expression (**B**) in naïve $CD4^+$ T cells, T_H0 cells and polarized T_H cells were analyzed by RT-qPCR. (**C** and **D**) Mouse naïve $CD4^+$ T cells were transfected with agomir-210 (**C**, n=3), antagomir-210 (**D**, n=3) or their corresponding controls and then differentiated into T_H1, T_H2, T_H17 and iT_{reg} cells for five days. The percentage of T_H1, T_H2, T_H17 and iT_{reg} cells was detected by flow cytometry. Statistical analysis data for the percentage of T_H1, T_H2, T_H17 and iT_{reg} cells were shown in the lower panel. All flow cytometry figures represent one set of experiments, and each experiment was repeated at least three times on different individuals. All data are obtained from C57BL/6J mice and represent the mean ± SEM. **P* < 0.05, ***P* < 0.01, ****P* < 0.001, NS: not significant. One-way ANOVA with Dunnett *post hoc* test (**A** and **B**) or two-tailed unpaired Student's *t*-test (**C** and **D**) were used.

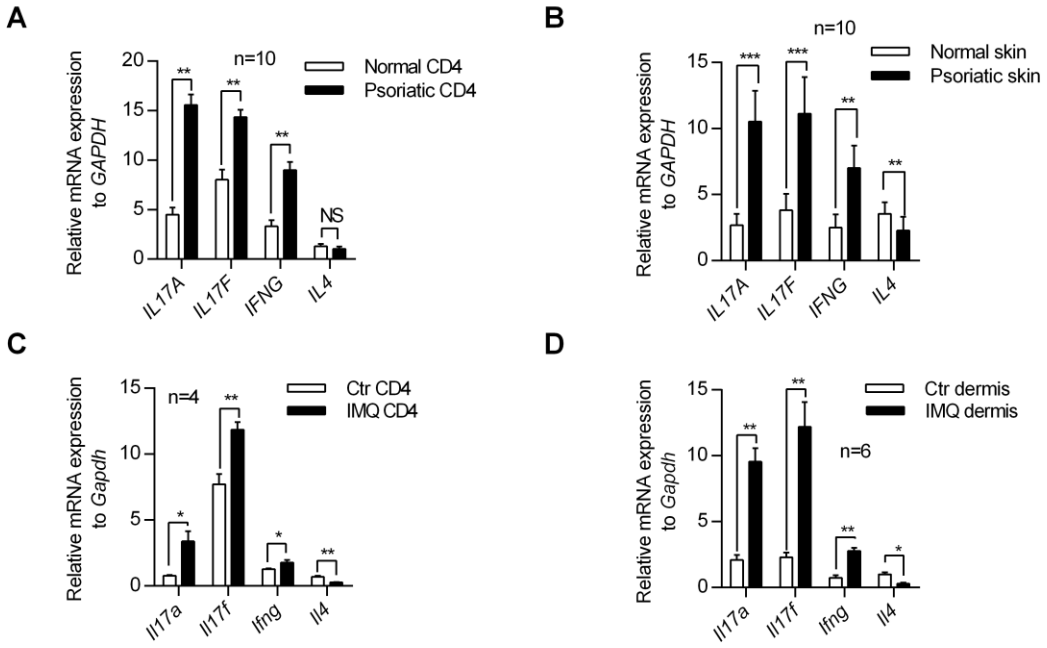

Supplemental Figure 8. Abnormal cytokine expression in psoriatic CD4$^+$ T cells and skin lesions. (**A** and **B**) The mRNA levels of *IL17A*, *IL17F*, *IFNG* and *IL4* in CD4$^+$ T cells (**A**, n=10) and skin samples (**B**, n=10) from healthy controls and psoriasis patients were determined by RT-qPCR. (**C** and **D**) The mRNA levels of *Il17a*, *Il17f*, *Ifng* and *Il4* in splenic CD4$^+$ T cells (**C**, n=4) and dermis (**D**, n=6) from untreated mice (Ctr) and IMQ-treated mouse (IMQ) were assessed by RT-qPCR. Data (**C** and **D**) are obtained from BALB/c mice and were representative of at least three independent experiments with three to six samples per group in each. Data represent the mean ± SEM. **P* < 0.05, ***P* < 0.01, ****P* < 0.001, NS: not significant. Two-tailed unpaired Student's *t*-test was used.

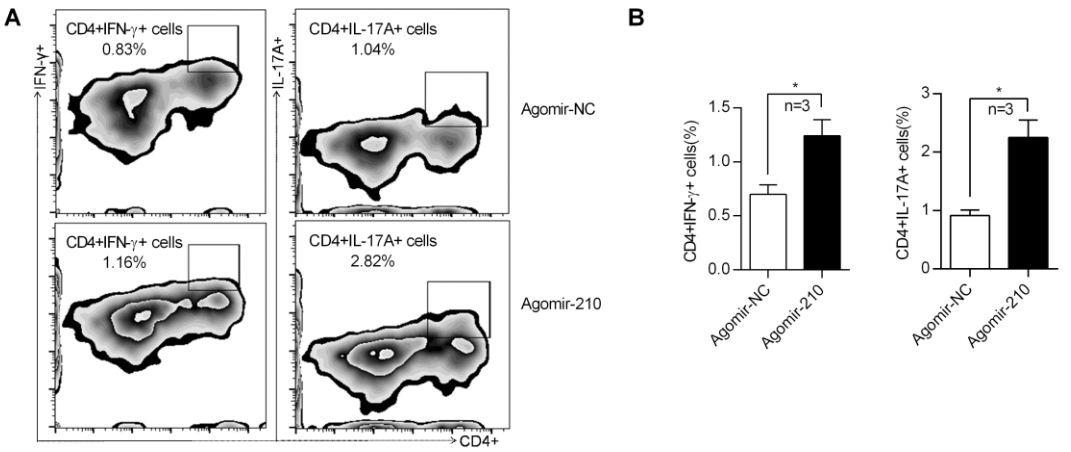

Supplemental Figure 9. miR-210 promotes the infiltration of T_H1 and T_H17 cells in dermis from IMQ-induced psoriasis-like mouse model. (**A**) Dermal single-cell suspensions were obtained from agomir-NC (n=3) and agomir-210 (n=3) treated IMQ mice on the 7th day. Then the cells were stained for T_H1 (CD4+IFN-γ+) and T_H17 (CD4+IL-17A+) cells and analyzed by flow cytometry. (**B**) Statistical analysis data for (**A**). All flow cytometry figures represent one set of experiments with three samples per group. All data are obtained from BALB/c mice and represent the mean ± SEM. **P* < 0.05. Two-tailed unpaired Student's *t*-test was used.

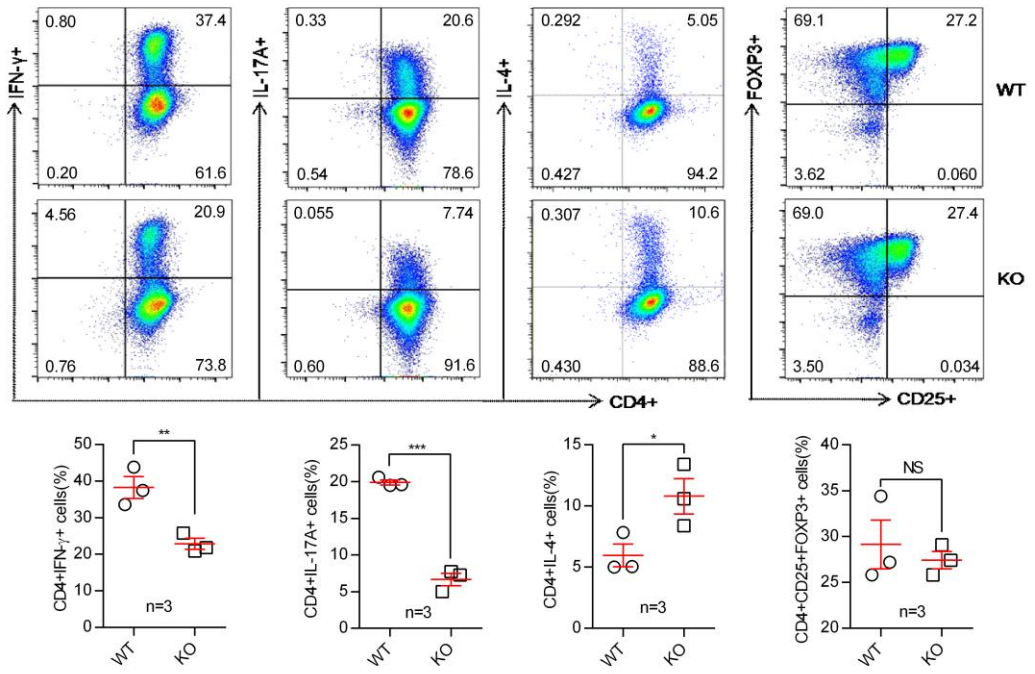

Supplemental Figure 10. T cell differentiation of naïve CD4$^+$ T cells from miR-210 KO mice. Naïve CD4$^+$ T cells were isolated from spleen of WT (n=3) and KO (n=3) mice and were then differentiated into T_H1, T_H2, T_H17 and iT_{reg} cells in vitro. The percentage of T_H1, T_H2, T_H17 and iT_{reg} cells was detected by flow cytometry (upper panel). Statistical data are shown in the lower panel. All flow cytometry figures represent one set of experiments, and each experiment was repeated at least three times. All data are obtained from miR-210 KO or WT mice with C57BL/6J background and represent the mean ± SEM. **P* < 0.05, ***P* < 0.01, ****P* < 0.001, NS: not significant. Two-tailed unpaired Student's *t*-test was used.

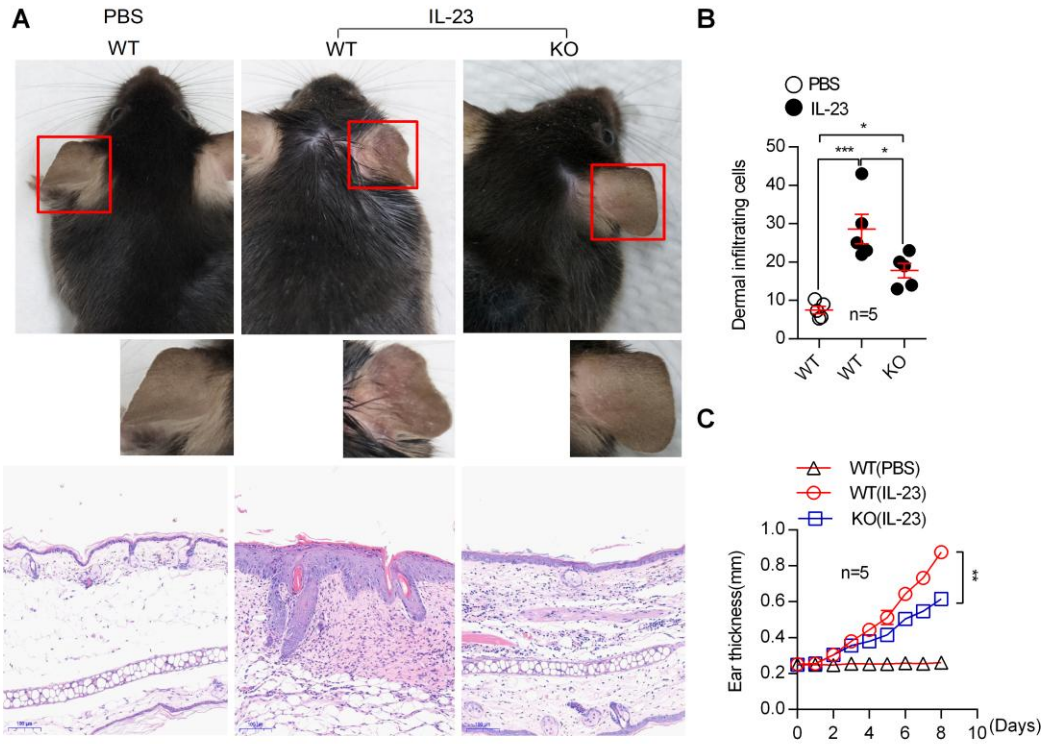

Supplemental Figure 11. miR-210 delation alleviates IL-23 induced psoriasis-like dermatitis. (**A**) Phenotypic presentation and H&E staining of mouse ears for WT or KO mice treated with IL-23 or PBS. Scale bar, 100 μm. (**B**) Dermal cellular infiltrates of mouse ears for IL-23-treated WT (n=5) and KO (n=5) mice as well as PBS-treated WT (n=5) mice. (**C**) Ear thickness of IL23-treated WT (n=5) and KO (n=5) mice as well as PBS-treated WT (n=5) mice were measured on the indicated days. All data are representative of at least three independent experiments with five samples per group in each. All data are obtained from miR-210 KO or WT mice with C57BL/6J background and represent the mean ± SEM. **P* < 0.05, ***P* < 0.01, ****P* < 0.001. One-way ANOVA (**C**) or with Bonferroni *post hoc* test (**B**) were used.

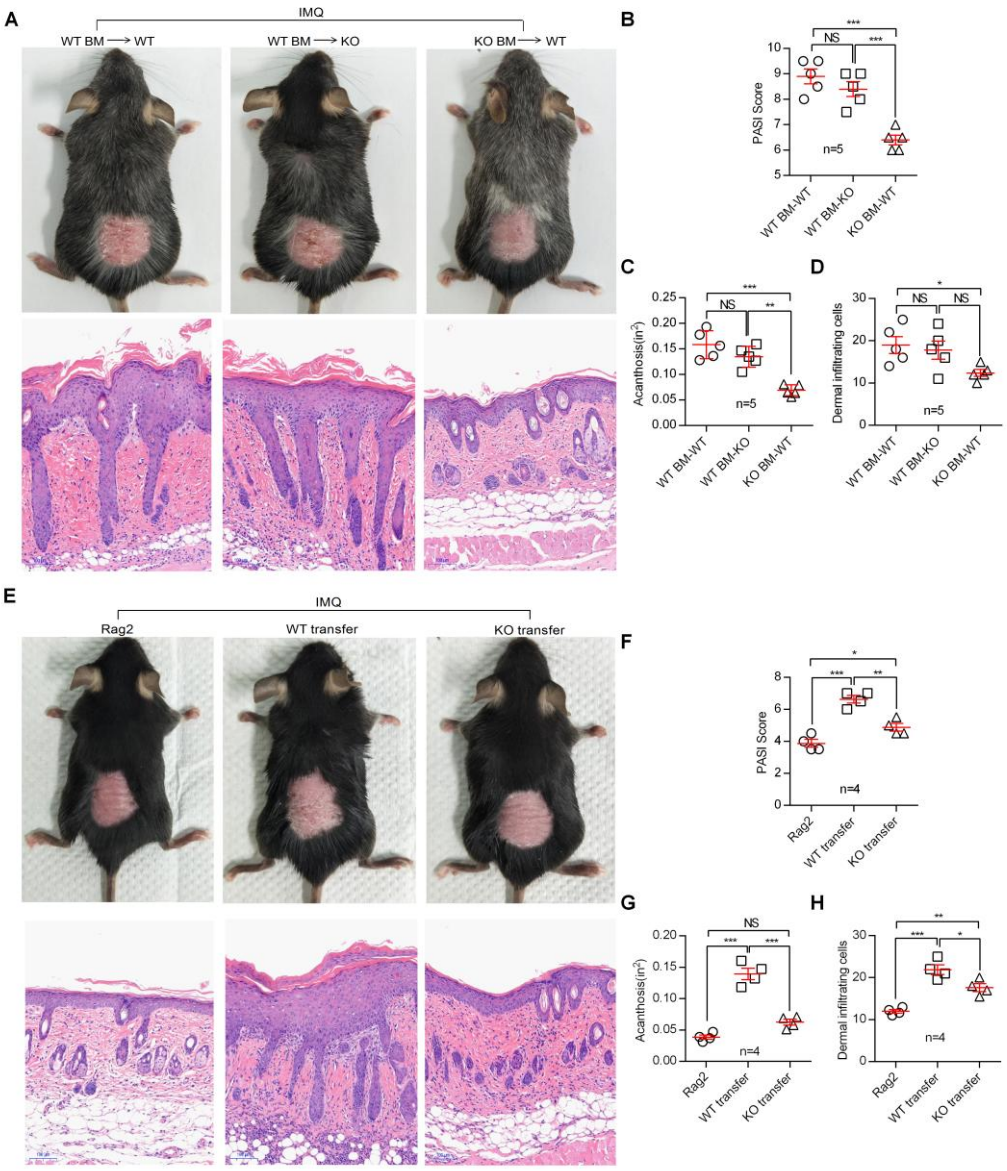

Supplemental Figure 12. miR-210 expression in CD4$^+$ T cells is pivotal for IMQ-induced psoriasis-like skin inflammation. (**A**) Lethally irradiated WT or miR-210 KO mice were adoptively transferred with miR-210 KO or WT bone marrow, and then the generated chimeric mice were subjected to IMQ-induced psoriasis-like mouse model. Representative phenotypic presentation and H&E staining of skin lesions derived from indicated groups, n=5 per group. Scale bar: 100μm. (**B**) PASI score of mice in (**A**), n=5 per group. (**C** and **D**) Acanthosis (**C**, n=5) and dermal cellular infiltrates (**D**, n=5) were quantitated for skin lesions derived from indicated groups. (**E**) *Rag2*$^{-/-}$ mice were transferred with naïve CD4$^+$ T cells derived from WT or miR-210 KO mice or not, then the mice were subjected to IMQ-induced psoriasis-like mouse model. Representative phenotypic presentation and H&E staining of skin lesions derived from indicated groups, n=4 per group. Scale bar: 100μm. (**F**) PASI score of mice in (**E**), n=4 per group. (**G** and **H**) Acanthosis (**G**, n=4) and dermal cellular infiltrates (**H**, n=4) were quantitated for skin lesions derived from indicated groups. Both miR-210 KO or WT mice and *Rag2*$^{-/-}$ mice have C57BL/6J background. Data represent the mean ± SEM. **P* < 0.05, ***P* < 0.01, ****P* < 0.001, NS: not significant. One-way ANOVA with Bonferroni *post hoc* test (**B-D** and **F-H**) was used.

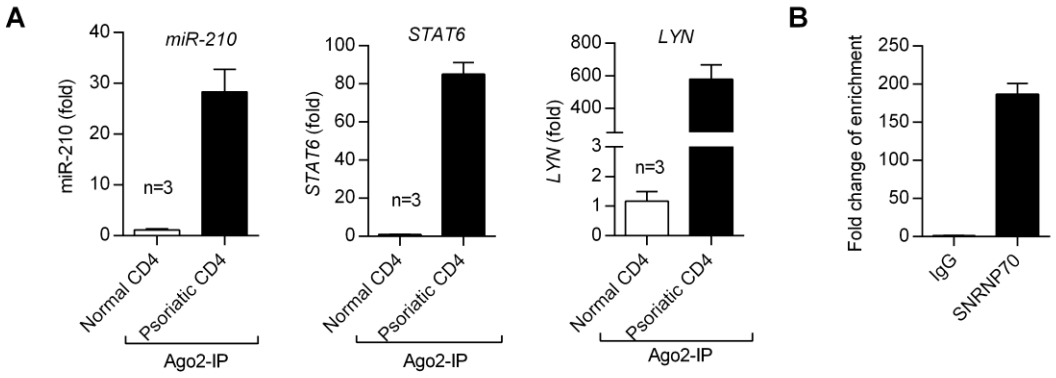

Supplemental Figure 13. RNA-binding protein immunoprecipitation (RIP) proves STAT6 and LYN as direct targets of miR-210. (**A**) Ago2-immunoprecipitates were assayed for mRNA levels of miR-210 (left panel), *STAT6* (middle panel) and *LYN* (right panel) in $CD4^+$ T cells lysates derived from healthy controls (n=3) or psoriasis patients (n=3). (**B**) *U1* expression was tested in SNRNP70 or IgG immunoprecipitates from normal $CD4^+$ T cell lysates, n=3 per group. All data are representative of at least three independent experiments. All data represent the mean ± SEM. Two-tailed unpaired Student's *t*-test was used.

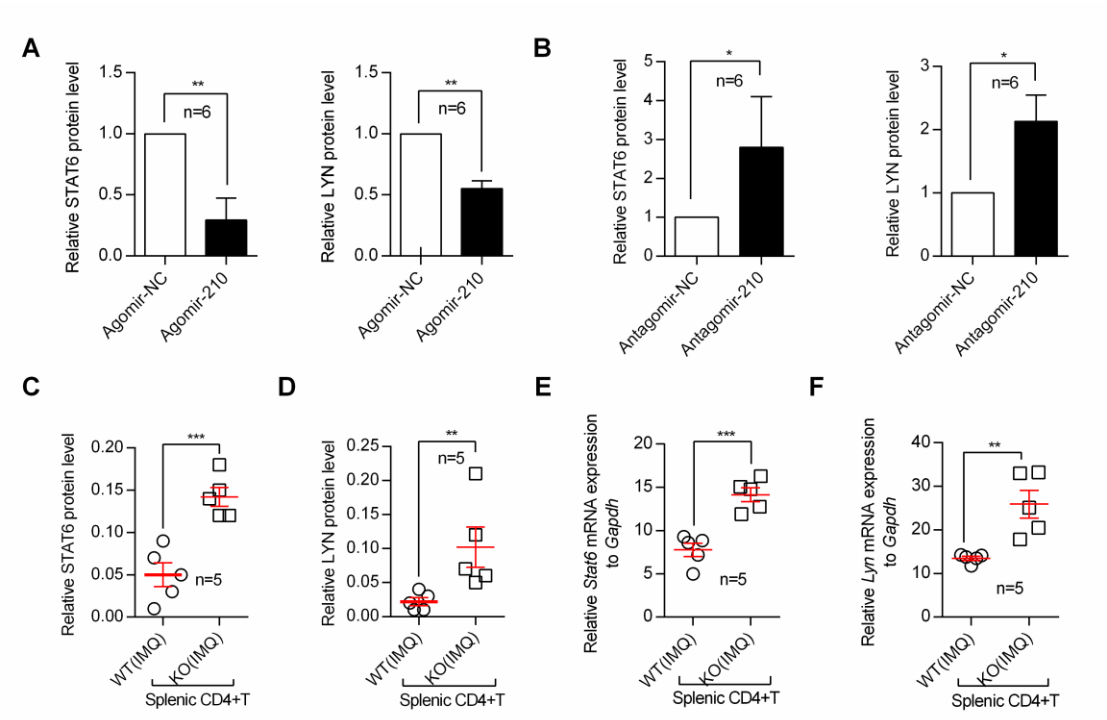

Supplemental Figure 14. miR-210 regulates the expression of STAT6 and LYN. (**A** and **B**) Statistical analysis data for STAT6 and LYN protein expression in Figure 6C, n=6 per group. (**C** and **D**) Statistical analysis data for STAT6 (**C**) and LYN (**D**) protein expression in Figure 6D, n=5 per group. (**E** and **F**) The mRNA levels of *Stat6* (**E**) and *Lyn* (**F**) were assessed by RT-qPCR in splenic $CD4^+$ T cells from IMQ-treated WT and KO mice, n=5 per group. Data (**C**-**F**) are obtained from miR-210 KO or WT mice with C57BL/6J background. All data represent the mean ± SEM. $*P < 0.05$, $**P < 0.01$, $***P < 0.001$. Two-tailed unpaired Student's *t*-test (**A**-**C** and **E**) or two-tailed Mann-Whitney *U*-test (**D** and **F**) were used.

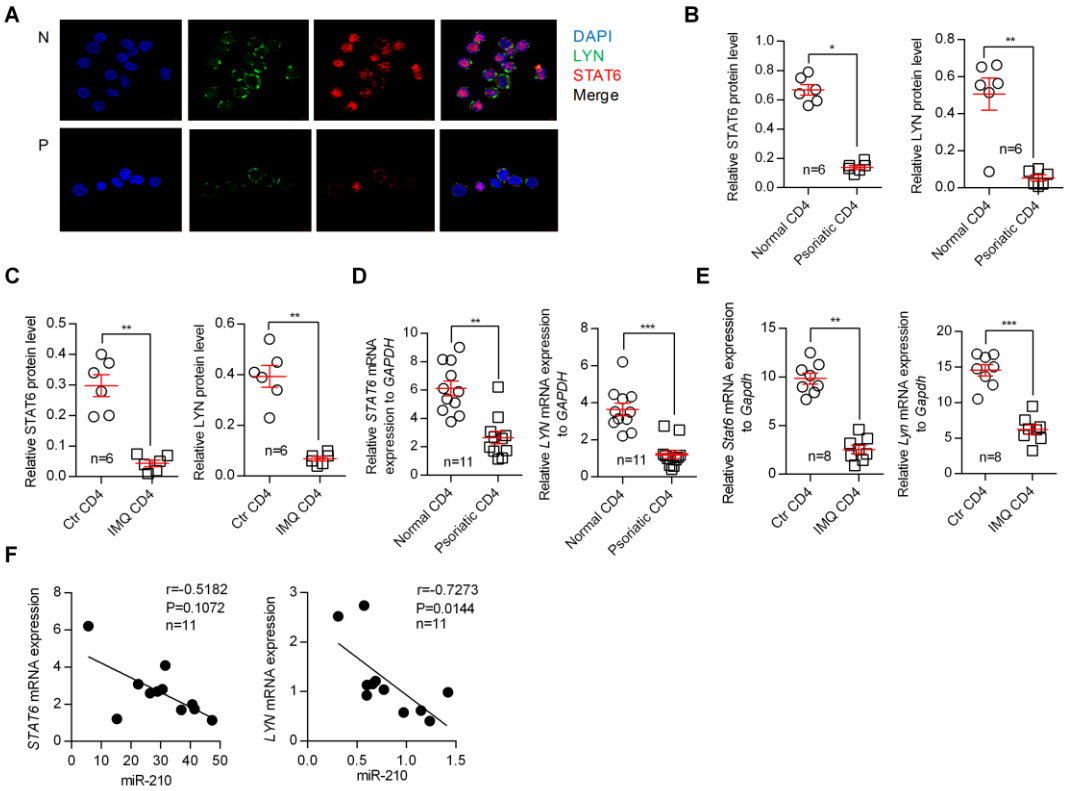

Supplemental Figure 15. The expression of STAT6 and LYN are decreased in psoriatic CD4$^+$ T cells. (**A**) The expression and subcellular localization of STAT6 and LYN in CD4$^+$ T cells from healthy individuals (N) and psoriasis patients (P). Red represents STAT6, green represents LYN, blue represents DAPI. (**B** and **C**) Statistical analysis data for STAT6 and LYN protein expression in Figure 6, E and F, n=6 per group. (**D** and **E**) *STAT6* and *LYN* mRNA expression was detected by RT-qPCR in CD4$^+$ T cells from psoriasis patients (**D**, n=11) and IMQ-induced psoriasis-like mouse model (**E**, n=8) as well as their healthy controls. (**F**) Correlation of *STAT6* (**F**, left panel, n=11) or *LYN* (**F**, right panel, n=11) mRNA expression with miR-210 expression in CD4$^+$ T cells from psoriasis patients. Data (**C** and **E**) were obtained from BALB/c mice. Data represent the mean ± SEM. $*P < 0.05$, $**P < 0.01$, $***P < 0.001$. Two-tailed Mann-Whitney *U*-test (**B** and **C**), two-tailed unpaired Student's *t*-test (**D** and **E**) or Spearman's *r*-test (**F**) were used.

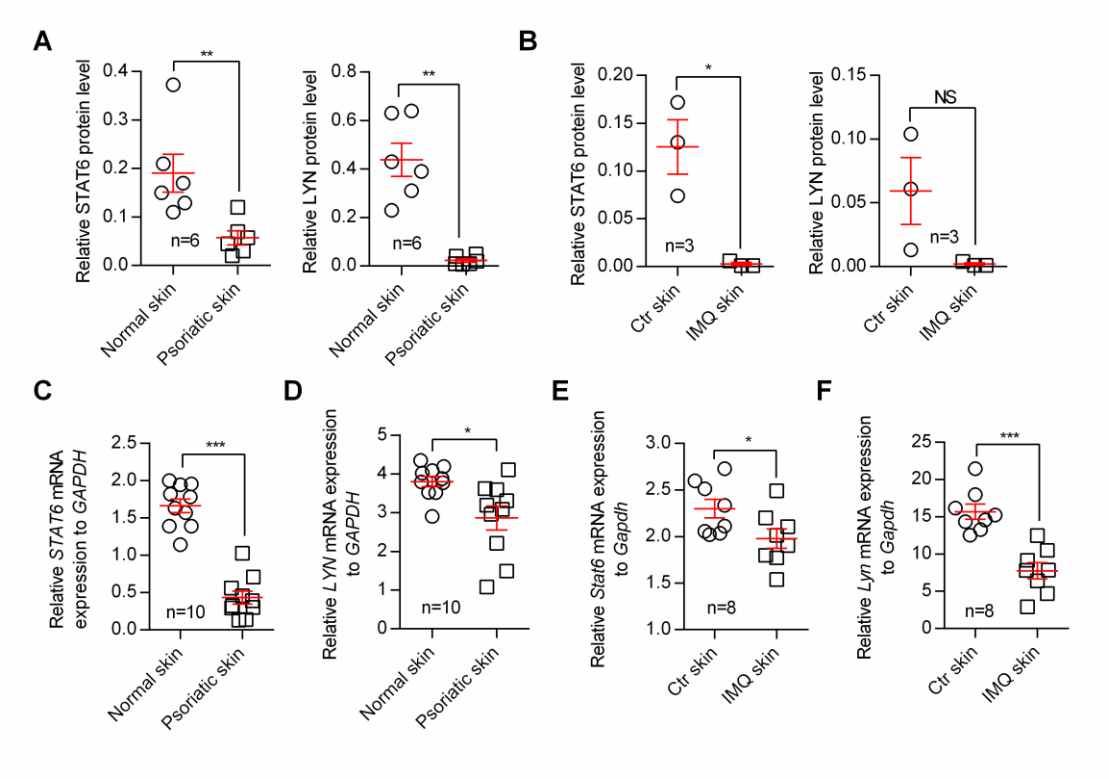

Supplemental Figure 16. The expression of STAT6 and LYN are decreased in psoriatic skin lesion. (**A**) Statistical analysis data for STAT6 and LYN protein expression in Figure 6G, n=6 per group. (**B**) Statistical analysis data for STAT6 and LYN protein expression in Figure 6H, n=6 per group. (**C-F**) *STAT6* and *LYN* mRNA expression was detected by RT-qPCR in skin lesions from psoriasis patients (**C** and **D**, n=10 per group) and IMQ-induced psoriasis-like mouse model (**E** and **F**, n=10 per group) as well as their healthy controls. Data (**B, E** and **F**) were obtained from BALB/c mice. Data represent the mean ± SEM. **P* < 0.05, ***P* < 0.01, ****P* < 0.001, NS: not significant. Two-tailed Mann-Whitney *U*-test (**A**, **B** and **D**) or two-tailed unpaired Student's *t*-test (**C**, **E** and **F**) were used.

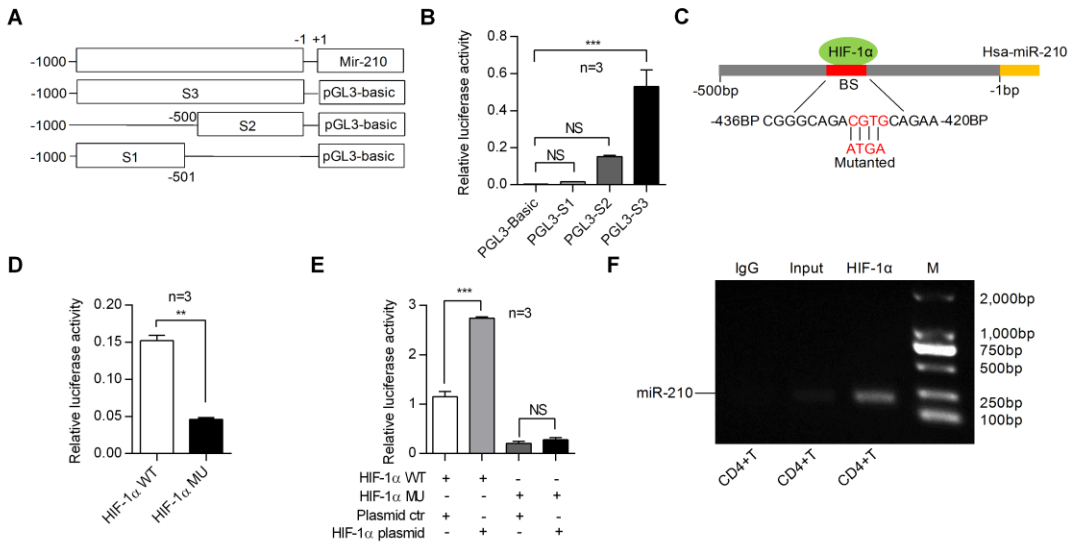

Supplemental Figure 17. HIF-1α binds to the miR-210 promoter. (**A** and **B**) Schematic representation of the proximal 1 kb of the miR-210 promoter, including the indicated reporter constructs (pGL3-basic) containing the full-length promoter (pGL3-S3) and additional truncation variants (pGL3-S2 and pGL3-S1) (**A**). Reporter constructs were transfected into HEK293T cells, and luciferase activity was detected (**B**, n=3 per group). S1:-501~-1000 bp; S2:-1~-500 bp; S3:-1~-1000 bp. (**C**) The structure diagram for predicted HIF-1α binding site (BS) in S2 area of miR-210 promoter region. (**D**) Luciferase activity was detected in HEK293T cells that were transfected with the recombinant plasmid HIF-1α WT (n=3) or a reporter construct with point-mutated HIF-1α BS in S2 (HIF-1α MU, n=3). (**E**) Luciferase activity was detected in HEK293T cells co-transfected with HIF-1α WT or HIF-1α MU and plasmid control or HIF-1α overexpression plasmid, n=3 per group, +: added; -: not added. (**F**) HIF-1α binds to the miR-210 promoter region. $CD4^+$ T cell lysates derived from psoriasis patients were used to perform chromatin immunoprecipitation (ChIP) assays. M, marker. Data (**B, D** and **E**) are representative of at least three independent experiments with three samples per group in each. Data represent the mean ± SEM. $^{**}P < 0.01$, $^{***}P < 0.001$, NS: not significant. One-way ANOVA with Dunnett *post hoc* test (**B**) or two-tailed unpaired Student's *t*-test (**D** and **E**) were used.

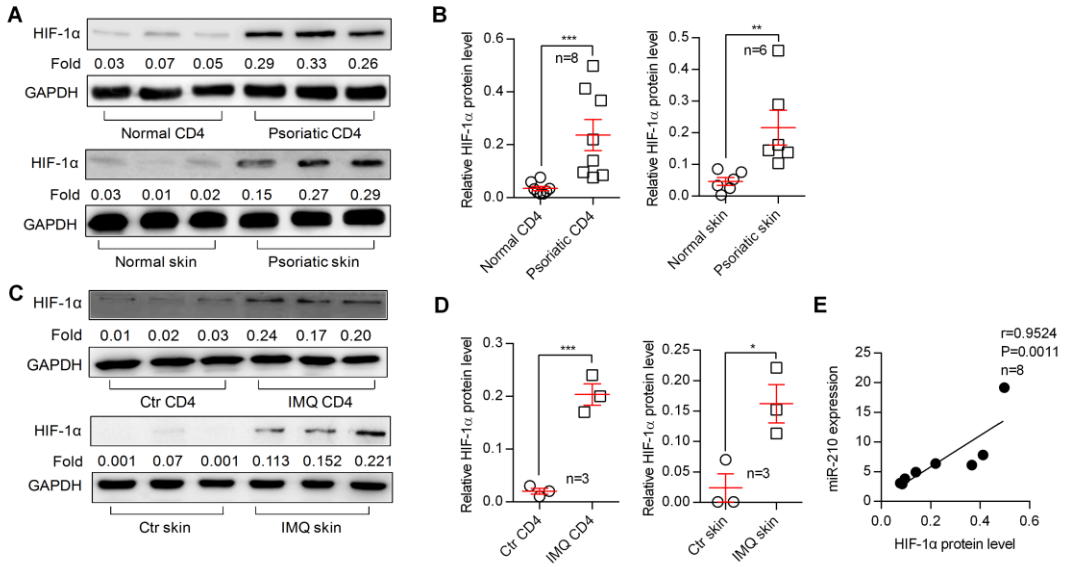

Supplemental Figure 18. HIF-1α expression is increased in psoriatic CD4$^+$ T cells and skin lesions. (**A** and **B**) Western blotting analysis of HIF-1α expression in CD4$^+$ T cells (n=8) and skin lesions (n=6) from healthy controls and psoriasis patients. Statistical analysis data for HIF-1α protein expression were shown in (**B**). (**C** and **D**) Western blotting analysis of HIF-1α expression in splenic CD4$^+$ T cells (n=3) and skin lesions (n=3) derived from untreated mice (Ctr) and IMQ-treated mice (IMQ). Statistical analysis data for HIF-1α protein expression were shown in (**D**). (**E**) Correlation of HIF-1α protein level and miR-210 expression in CD4$^+$ T cells from psoriasis patients, n=8. Data (**C** and **D**) were obtained from BALB/c mice. Data represent the mean ± SEM. **P* < 0.05, ***P* < 0.01, ****P* < 0.001. Two-tailed Mann-Whitney *U*-test (**B**), two-tailed unpaired Student's *t*-test (**D**) or Spearman's *r*-test (**E**) were used.

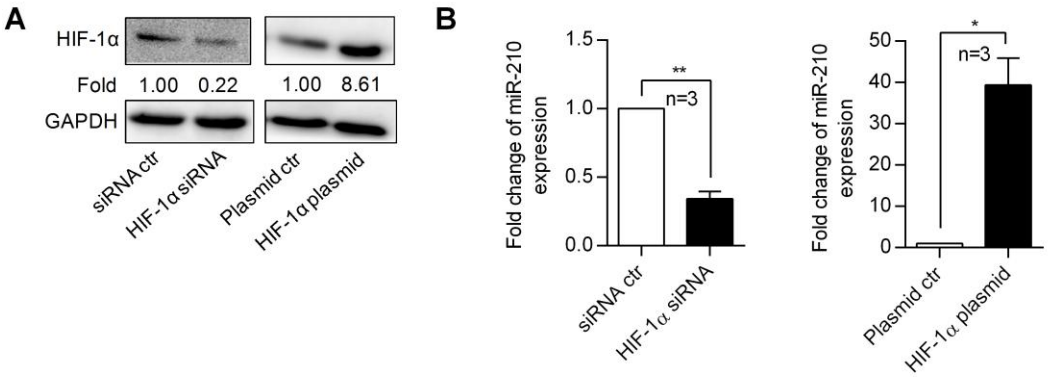

Supplemental Figure 19. HIF-1α regulates the expression of miR-210. (**A** and **B**) $CD4^+$ T cells from psoriasis patients were transfected with HIF-1α siRNA (n=3), and normal human $CD4^+$ T cells were transfected with the HIF-1α overexpression plasmid (n=3) for 2 days. Then, cells were collected to detect HIF-1α protein level (**A**) and miR-210 expression level (**B**). Data represent the mean ± SEM. **P* < 0.05, ***P* < 0.01. Two-tailed unpaired Student's *t*-test was used.

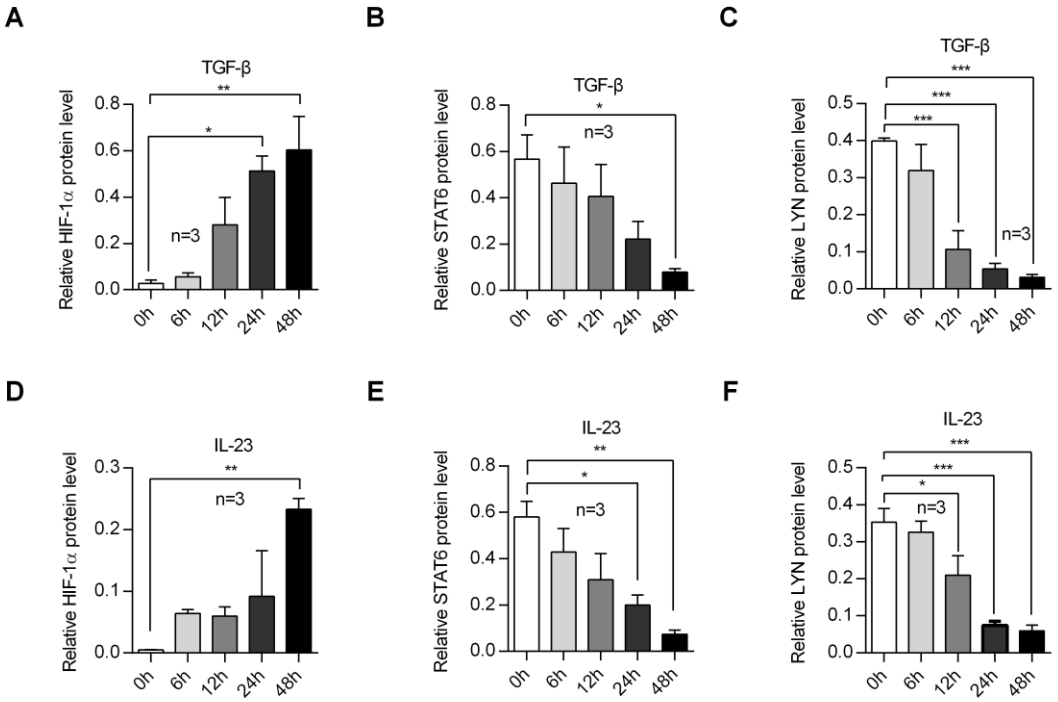

Supplemental Figure 20. The statistical analysis data for HIF-1α, STAT6 and LYN protein expression in Figure 8B. N=3 per group. Data represent the mean ± SEM. **P* < 0.05, ***P* < 0.01, ****P* < 0.001. One-way ANOVA with Dunnett *post hoc* test was used.

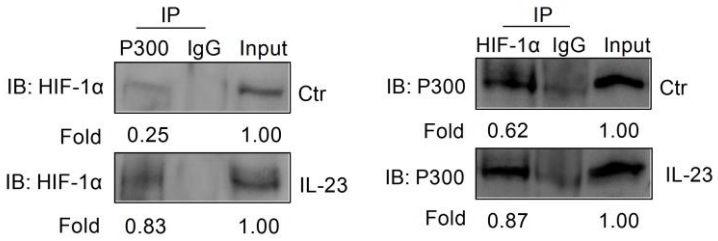

Supplemental Figure 21. IL-23 promotes the interaction between HIF-1α and P300. Normal $CD4^+$ T cells were stimulated with or without IL-23 (20 ng/ml) for 48h. Then P300 (left panel) or HIF-1α (right panel) was immunoprecipitated and analyzed by western blot using antibodies against the proteins indicated on the left of each panel. The data is representative of at least three independent experiments.

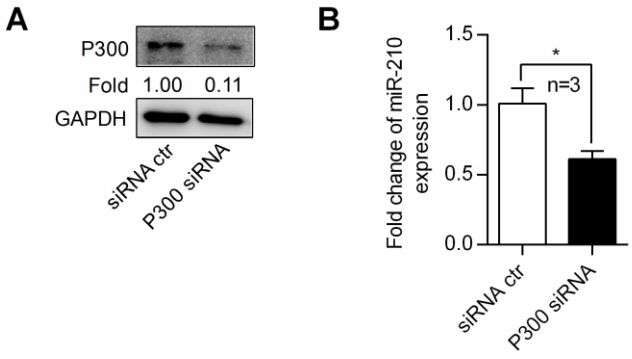

Supplemental Figure 22. P300 affects the expression of miR-210 in CD4$^+$ T cells. The protein levels of P300 (**A**) and miR-210 expression (**B**) in psoriatic CD4$^+$ T cells transfected with P300 siRNA (n=3) or siRNA control (n=3). Data represent the mean ± SEM. *$P < 0.05$. Two-tailed unpaired Student's *t*-test (**B**) was used.

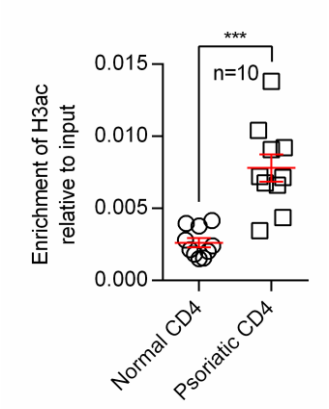

Supplemental Figure 23. The histone H3 acetylation (H3ac) levels on the miR-210 promoter was increased in psoriatic CD4$^+$ T cells. The H3ac levels on the miR-210 promoter in CD4$^+$ T cells from psoriasis patients (n=10) and normal controls (n=10). Data represent the mean ± SEM. ***P < 0.001. Two-tailed Mann-Whitney U-test was used.

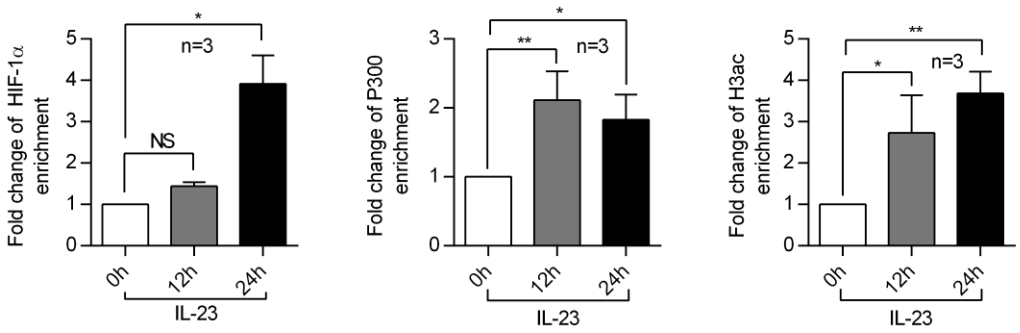

Supplemental Figure 24. IL-23 increases the level of H3ac on miR-210 promoter by inducing the combination of HIF-1α and P300. The enrichments of HIF-1α, P300 and H3ac on the miR-210 promoter in normal $CD4^+$ T cells stimulated with IL-23, n=3 per group. Data represent the mean ± SEM. **P* < 0.05, ***P* < 0.01, NS: not significant. One-way ANOVA with Dunnett *post hoc* test was used.

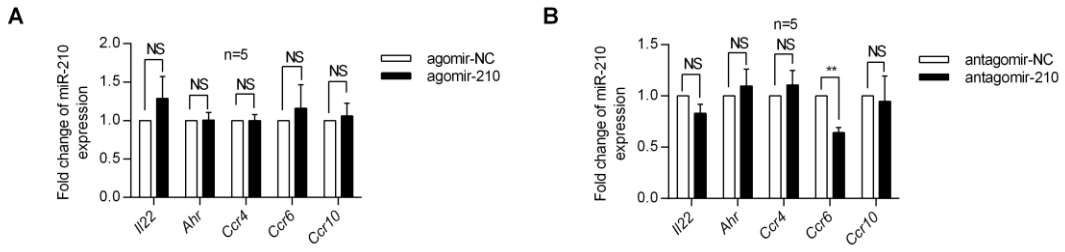

Supplemental Figure 25. miR-210 has no obvious effect on the mRNA expression of T_H22 related genes in vivo. (**A** and **B**) The mRNA levels of *Il22*, *Ahr*, *Ccr4*, *Ccr6 and Ccr10* in splenic $CD4^+$ T cells from IMQ-induced mice injected with agomir-210/agomir-NC (**A**, n=5) or antagomir-210/antagomir-NC (**B**, n=5) on the 7th day. Data are obtained from BALB/c mice and represent the mean ± SEM. ***P* < 0.01, NS: not significant. Two-tailed unpaired Student's *t*-test was used.

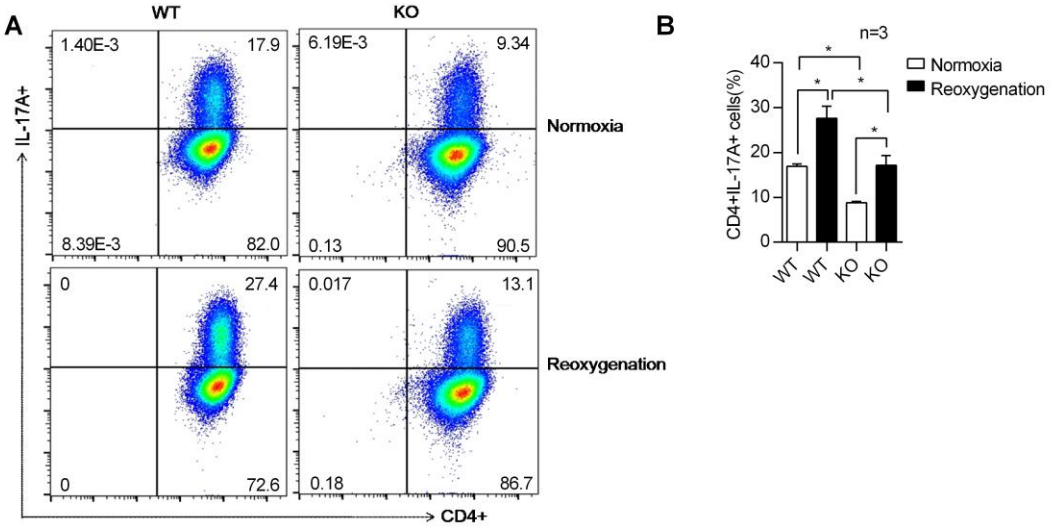

Supplemental Figure 26. The effect of miR-210 on T_H17 cell differentiation under normoxia or reoxygenation. (**A** and **B**) Naïve $CD4^+$ T cells were sorted from the spleens of WT and KO mice, and cells were stimulated with 2 μg/ml plate-bound anti-CD3 and 2 μg/ml soluble anti-CD28 under T_H17-skewing conditions (10 μg/ml anti-IL-4, 10 μg/ml anti-IFN-γ, 2 ng/ml TGF-β and 0.2 ng/ml IL-6) for three days. For the reoxygenation assay, T cells were first primed under a low O_2 concentration (5% O_2) for 36 h, and the cells were then transferred into a normoxic incubator for the rest of the culture. The differentiated cells were analyzed by flow cytometry for cytokine production by intracellular staining of IL-17A (**A**). The statistical analysis data are shown in (**B**), n=3 per group. All data are obtained from miR-210 KO or WT mice with C57BL/6J background and represent the mean ± SEM. **P* < 0.05, ****P* < 0.001, NS: not significant. One-way ANOVA with Bonferroni *post hoc* test was used.

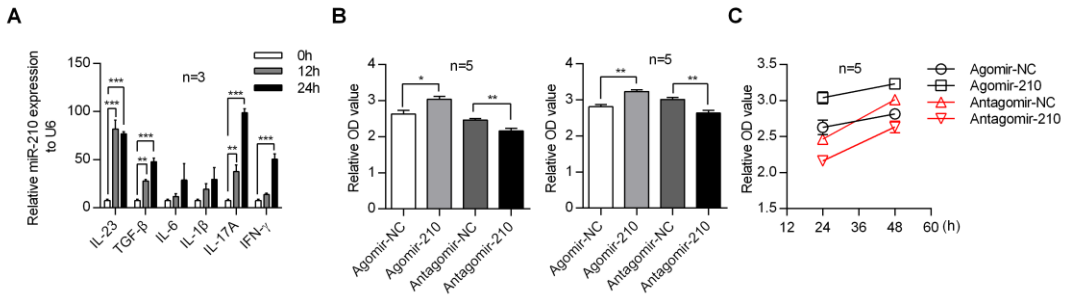

Supplemental Figure 27. miR-210 promotes the proliferation of keratinocytes. (**A**) HaCaT cells were stimulated with IL-23 (20 ng/ml), TGF-β (5 ng/ml), IL-6 (10 ng/ml), IL-1β (10 ng/ml), IL-17A (200 ng/ml) and IFN-γ (200 ng/ml). Cells were collected to detect the expression of miR-210 at 0h, 12h and 24h. N=3 per group. (**B**) Normal human epidermal keratinocytes (NHEKs) were transfected with agomir-210 or antagomir-210 as well as their corresponding controls for 24 h (left panel, n=5 per group) and 48 h (right panel, n=5 per group). Then the proliferation of keratinocytes was analyzed by CCK8 assay. (**C**) The tendency of keratinocyte proliferation in (**B**). Data (**A-C**) are representative of at least three independent experiments with five samples per group in each. Data represent the mean ± SEM. **P* < 0.05, ***P* < 0.01, ****P* < 0.001, NS: not significant. One-way ANOVA with Dunnett *post hoc* test (**A**) or two-tailed unpaired Student's *t*-test (**B**) were used.

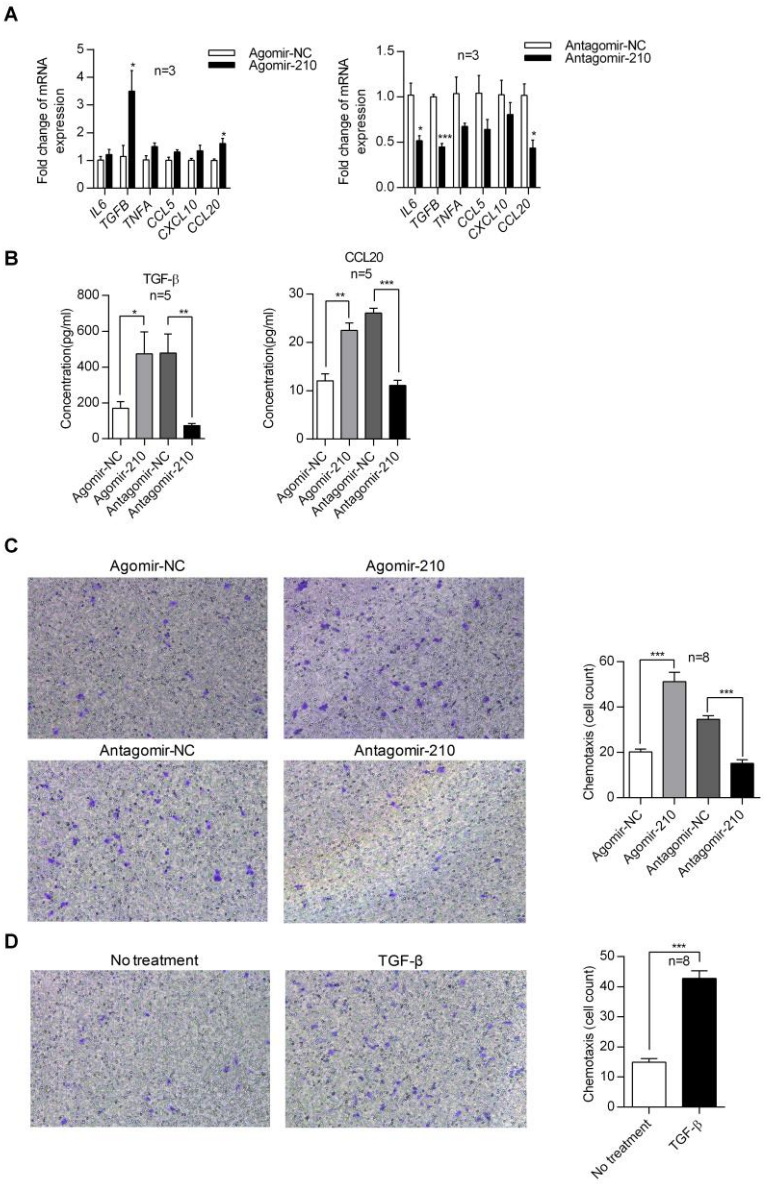

Supplemental Figure 28. miR-210 promotes the chemotaxis of keratinocytes to CD4$^+$ T cells. (**A**) NHEKs were transfected with agomir-210 (left panel, n=3), antagomir-210 (right panel, n=3) and their corresponding controls for 48 h. Then, cells were collected to detect the mRNA levels of cytokines and chemokines secreted by keratinocytes. (**B**) The cell supernatant was collected to detect the secretion of TGF-β (left panel, n=5) and CCL20 (right panel, n=5) by ELISA. (**C** and **D**) NHEKs were transfected with agomir-210, antagomir-210 and their corresponding controls (C, n=8) or stimulated with TGF-β (5 ng/ml) (D, n=8) for 48 h. Then, the culture supernatants were collected and added to the lower chambers, and normal human CD4$^+$ T cells were added to the upper chambers of transwell plates for 90 min. The upper chamber was removed and stained with crystal violet, and cells were counted. Data represent the mean ± SEM. **P* < 0.05, ***P* < 0.01, ****P* < 0.001, NS: not significant. Two-tailed unpaired Student's *t*-test was used.

Supplemental Table 1. Information for patients with psoriasis vulgaris

Sample ID	Age/ Gender	PASI score	Sample ID	Age/ Gender	PASI score	Sample ID	Age/ Gender	PASI score
1	50/M	20.6	**22**	36/F	0.7	**43**	22/M	8.2
2	51/M	7.8	**23**	19/F	0.7	**44**	18/F	2.4
3	31/M	17.8	**24**	25/F	9.5	**45**	31/F	5.6
4	53/F	3.9	**25**	24/F	8.6	**46**	29/F	12.9
5	30/F	25.3	**26**	38/M	13.4	**47**	38/F	8.1
6	40/M	6.7	**27**	54/M	10.6	**48**	21/M	2.5
7	41/M	17.4	**28**	40/M	11.8	**49**	42/M	10.4
8	55/F	7.2	**29**	56/M	10.2	**50**	46/M	19.8
9	36/M	3.3	**30**	30/M	0.2	**51**	25/M	5.2
10	20/M	29.2	**31**	29/M	2.4	**52**	26/F	12.0
11	34/M	24.0	**32**	45/M	5.9	**53**	20/F	6.4
12	43/M	6.9	**33**	22/M	18.1	**54**	26/M	11.0
13	46/M	10.2	**34**	31/M	10.7	**55**	53/M	12.0
14	53/M	18.3	**35**	45/M	8.0	**56**	50/F	13.6
15	21/M	11.6	**36**	30/M	4.0	**57**	43/M	11.1
16	50/F	12.8	**37**	42/F	4.5	**58**	28/F	17.7
17	44/M	13.2	**38**	48/M	8.8	**59**	26/M	9.0
18	54/M	2.5	**39**	27/M	8.9	**60**	52/F	10.6
19	45/M	10.7	**40**	30/M	12.5	**61**	23/M	9.3
20	26/M	13.4	**41**	63/M	27.2	**62**	23/M	20.4
21	37/M	8.9	**42**	20/M	10.4	**63**	32/F	19.2

All patients were clinically diagnosed as psoriasis vulgaris. M, male; F, female; PASI: psoriasis area and severity index.

Supplemental Table 2. Primer sequences and siRNA sequences.

Quantitative PCR primers	
Human-*STAT6*-F	5′-GGAGCACCATCTTGCAACAC-3′
Human-*STAT6*-R	5′-GTGGCGGAACTGTTCCATAA-3′
Human-*LYN*-F	5′-ATGTGAGAGATCCAACGTCCAA-3′
Human-*LYN*-R	5′-AAAAGCTGCCTTTCTGCGTC-3′
Human-*IL4*-F	5′-GGTCACAGGAGAAGGGACGCC-3′
Human-*IL4*-R	5′-TGCGAAGCACCTTGGAAGCCC-3′
Human-*IFNG*-F	5′-CATCCAAAAGAGTGTGGAGACA-3′
Human-*IFNG*-R	5′-TGCTTTGCGTTGGACATTCAAG-3′
Human-*IL17A*-F	5′-ATTACTACAACCGATCCACCTC-3′
Human-*IL17A*-R	5′-TGGTAGTCCACGTTCCCAT-3′
Human-*IL17F*-F	5′-AGTAAGCCACCAGCGCAACATG-3′
Human-*IL17F*-R	5′-CTCAGAAAGGCAAGCCCCAATA-3′
Human-*IL6*-F	5′-AATTCGGTACATCCTCGACGGC-3′
Human-*IL6*-R	5′-GCCAGTGCCTCTTTGCTGCTTT-3′
Human-*TNFA*-F	5′-GGACACCATGAGCACTGAAAGC-3′
Human-*TNFA*-R	5′-TGCCACGATCAGGAAGGAGAAG-3′
Human-*TGFB*-F	5′-GCAACAATTCCTGGCGATAC-3′
Human-*TGFB*-R	5′-AAGGCGAAAGCCCTCAAT-3′
Human-*TBX21*-F	5′-CAGGGACGGCGGATGTTCC-3′
Human-*TBX21*-R	5′-TCCACACTGCACCCACTTGC-3′
Human-GATA3-F	5′-ACAGAACCGGCCCCTCATTAA-3′
Human-GATA3-R	5′-TGGTCTGACAGTTCGCACAGGA-3′
Human-*RORC*-F	5′-AGGCCATTCAGTACGTGGTGGA-3′
Human-*RORC*-R	5′-CGTGCGGTTGTCAGCATTGTAG-3′
Human-*FOXP3*-F	5′-CTTTCACCTACGCCACGCTCAT-3′
Human-*FOXP3*-R	5′-TCCAGGTGGCAGGATGGTTTCT-3′

Human-*CCL20*-F	5′-ATTGTGCGTCTCCTCAGTAAAAA-3′
Human-*CCL20*-R	5′-TGTGATGCTTAAACAAAGCAAAC-3′
Human-*CCL5*-F	5′-CAGTCGTCTTTGTCACCCGA-3′
Human-*CCL5*-R	5′-TGTAACTGCTGCTGTGTGGT-3′
Human-*CXCL10*-F	5′-AACTGTACGCTGTACCTGCAT-3′
Human-*CXCL10*-R	5′-GCATCGATTTTGCTCCCCTC-3′
Human-*GAPDH*-F	5′-ATGGGGAAGGTGAAGGTCG-3′
Human-*GAPDH*-R	5′-GGGGTCATTGATGGCAACAATA-3′
Mouse-*Stat6*-F	5′-GAGTTCCTGGTCGGTTCAGA-3′
Mouse-*Stat6*-R	5′-GCTCTCCAAGGTGCTGATGT-3′
Mouse-*Lyn*-F	5′-CGGCTGCTTCACTATCAAATCTG-3′
Mouse-*Lyn*-R	5′-CTCATCACATCTGCGTTGGTTC-3′
Mouse-*Il4*-F	5′-CATATCCACGGATGCGACAA-3′
Mouse-*Il4*-R	5′-CGTCCTCACAGCAACGAAGA-3′
Mouse-*Ifng*-F	5′-AGACAATCAGGCCATCAGCA-3′
Mouse-*Ifng*-R	5′-CAACAGCTGGTGGACCACTC-3′
Mouse-*Il17a*-F	5′-ATGCTGTTGCTGCTGCTGAG-3′
Mouse-*Il17a*-R	5′-GGAAGTCCTTGGCCTCAGTG-3′
Mouse-*Il17f*-F	5′-GGAGGTAGCAGCTCGGAAGA-3′
Mouse-*Il17f*-R	5′-GGAGCGGTTCTGGAATTCAC-3′
Mouse-*Il22*-F	5′-ATGAGTTTTTCCCTTATGGGGAC-3′
Mouse-*Il22*-R	5′-GCTGGAAGTTGGACACCTCAA-3′
Mouse-*Ahr*-F	5′-AGCCGGTGCAGAAAACAGTAA-3′
Mouse-*Ahr*-R	5′-AGGCGGTCTAACTCTGTGTTC-3′
Mouse-*Ccr4*-F	5′-GGAAGGTATCAAGGCATTTGGG-3′
Mouse-*Ccr4*-R	5′-GTACACGTCCGTCATGGACTT-3′
Mouse-*Ccr6*-F	5′-CCTGGGCAACATTATGGTGGT-3′
Mouse-*Ccr6*-R	5′-CAGAACGGTAGGGTGAGGACA-3′

Mouse-*Ccr10*-F	5′-GGACTTTACTCCGGGTACGAT-3′
Mouse-*Ccr10*-R	5′-CAGGGAGACACTGGGTTGGA-3′
Mouse-*Tbx21*-F	5′-CAACAACCCCTTTGCCAAAG-3′
Mouse-*Tbx21*-R	5′-TCCCCCAAGCAGTTGACAGT-3′
Mouse-*Gata3*-F	5′-AGAACCGGCCCCTTATGAA-3′
Mouse-*Gata3*-R	5′-AGTTCGCGCAGGATGTCC-3′
Mouse-*Rorc*-F	5′-GGACAGGGAGCCAAGTTCTCA-3′
Mouse-*Rorc*-R	5′- CACAGGTGATAACCCCGTAGTGG-3′
Mouse-*Foxp3*-F	5′-TTGCCAAGCTGGAAGACTGC-3′
Mouse-*Foxp3*-R	5′-CAGACGGTGCCACCATGACT-3′
Mouse-*Gapdh*-F	5′-AGGTCGGTGTGAACGGATTTG-3′
Mouse-*Gapdh*-R	5′-TGTAGACCATGTAGTTGAGGTCA-3′
RIP primers	
Human-*STAT6*-RIP-F	5′-GGAAGGGAAGTTCAGGCTCT-3′
Human-*STAT6*-RIP-R	5′-ATGCCCTAACCTGTGCTCTT-3′
Human-*LYN*-RIP-F	5′-GCCTTGTTTTGCTTCTCCCA-3′
Human-*LYN*-RIP-R	5′-CTTCCACACATGCTGGACAC-3′
ChIP-qPCR primers	
Forword primer	5′-GGAAATTGGCAGGACTGGG-3′
Reverse primer	5′-GCCTCTAAGAGT CAGTGGGG-3′
siRNA sequences	
Human-STAT*6*-siRNA-sense	5′-CAUGAGCAUGCAGCUUGGCCCAGAU-3′
Human-STAT6-siRNA-anti-sense	5′-AUCUGGGCCAAGCUGCAUGCUCAUG-3′
Human-LYN-siRNA-sense	5′-CCUGUAUCAGCGACAUGAUUAAACA-3′
Human-LYN-siRNA-anti-sense	5′-UGUUUAAUCAUGUCGCUGAUACAGG-3′
Human-HIF-1α-siRNA-sense	5′-GAAAUUCCUUUAGAUAGCAAGACUU-3′
Human- HIF-1α-siRNA-anti-sense	5′-AAGUCUUGCUAUCUAAAGGAAUUUC-3′
Human-P300-siRNA-sense	5′-CAGGUAUGAUGAACAGUCCAGUAAA-3′

Human-P300-siRNA-anti-sense	5′-UUUACUGGACUGUUCAUCAUACCUG-3′

1

2

Supplemental Table 3. Potential target genes of hsa-miR-210-3p predicted by bioinformatic tools.

Gene	miRWalk	miRanda	RNA22	Targetscan
STAT6	1	1	1	1
LYN	1	1	0	1
SPRED2	1	1	1	1
CEND1	1	1	1	1
MFSD4	1	1	1	1
FLNC	1	1	1	1
GGNBP2	1	1	0	1
MAB21L3	1	1	1	1
USH2A	1	1	1	1
ATXN1	1	1	1	1
B4GALT5	1	1	1	1
FOXD2	1	1	1	1
C3orf18	1	1	1	1
IGF2	1	1	1	1
ELOVL6	1	1	1	1
OXTR	1	1	1	1
SLCO4C1	1	1	1	1
DSC3	1	1	1	1
UPF1	1	1	1	1
ARHGAP35	1	1	1	1
ADAMTS5	1	1	1	1
SDF2	1	1	0	1
CCDC68	1	1	1	1
CNTNAP5	1	1	1	1
CUL3	1	1	1	1
KIAA0141	1	1	1	1
RGMA	1	1	1	1
CLEC16A	1	1	1	1
INHBB	1	1	1	1
CHRNB1	1	1	1	1
NR3C2	1	1	1	1
SIN3B	1	1	1	1
ZNF445	1	1	1	1
SMG5	1	1	1	1
RIT1	1	1	1	1
COX10	1	1	1	1
NSUN5	1	1	1	1
TMEM105	1	1	1	1
EFNA3	1	1	1	1
VAMP4	1	1	1	1
ZNF449	1	1	1	1
PPP1R2	1	1	1	1
SLC6A6	1	1	1	1
TOR1A	1	1	1	1
TSPAN10	1	1	1	1
FANCF	1	1	1	1
TTC9	1	1	1	1
TMEM40	1	1	1	1
ACVR1B	1	1	0	1

Gene	miRWalk	miRanda	RNA22	Targetscan
CACNA1C	1	1	0	1
TUSC5	1	1	1	1
TFRC	1	1	1	1
RAB9B	1	1	1	1
PRKCA	1	1	1	1
FKBP9	1	1	1	1
MEF2D	1	1	1	1
ADAMTS6	1	1	1	1
KIAA1755	1	1	1	1
MAPK1	1	1	1	1
MNT	1	1	1	1
KCNK5	1	1	1	1
ASCL1	1	1	1	1
THBS2	1	1	1	1
RAB3B	1	1	1	1
RAB7A	1	1	1	1
KCTD11	1	1	1	1
SLC1A2	1	1	1	1
TREML2	1	1	1	1
ALDH5A1	1	1	1	1
TPMT	1	1	1	1
POMT2	1	1	1	1
RAB27B	1	1	1	1
BMP6	1	1	1	1
DAK	1	1	1	1
TECPR2	1	1	1	1
TTC24	1	1	1	1
ICMT	1	1	1	1
MSANTD1	1	1	0	1
CAPN9	1	1	1	1
NT5DC1	1	1	1	1
TMEM204	1	1	1	1
C8orf86	1	1	1	1
E2F3	1	1	1	1
NPTX1	1	1	1	1
OTUB2	1	1	1	1
FAM196A	1	1	1	1
UCP3	1	1	1	1
MDGA1	1	1	1	1
GNA15	1	1	1	1
SUPT7L	1	1	1	1
PSAP	1	1	1	1
ACVR1B	1	1	0	1
ADCY5	1	1	1	1
ABCD1	1	1	0	1
ARRB1	1	1	0	1
ATP2B3	1	1	1	1
BARD1	1	1	0	1
BDKRB2	1	1	1	1
BICD1	1	1	0	1
BMP6	1	1	0	1
CACNA1A	1	1	1	1
CACNA1C	1	1	0	1
RUNX1T1	1	1	0	1

Gene	miRWalk	miRanda	RNA22	Targetscan
CCKBR	1	1	0	1
CD22	1	1	1	1
CHN1	1	1	0	1
CHRNB1	1	1	0	1
ACKR2	1	1	1	1
CSF1	1	1	1	1
CSNK1E	1	1	1	1
DRD5	1	1	0	1
DSC3	1	1	0	1
E2F3	1	1	0	1
EFNA3	1	1	0	1
CTTN	1	1	1	1
EPB41L1	1	1	1	1
F7	1	1	1	1
FLNC	1	1	0	1
GNAT1	1	1	0	1
ARHGAP35	1	1	0	1
TLX1	1	1	1	1
PRMT2	1	1	1	1
HTR5A	1	1	0	1
IGF2	1	1	0	1
INPP5A	1	1	1	1
KCNJ15	1	1	1	1
KIF5A	1	1	0	1
KIR2DL4	1	1	0	1
IPO5	1	1	1	1
LAIR1	1	1	0	1
LMX1B	1	1	1	1
SMAD4	1	1	1	1
MEF2C	1	1	0	1
MEF2D	1	1	0	1
MLLT1	1	1	0	1
NR3C2	1	1	0	1
ABCC1	1	1	0	1
MUC4	1	1	0	1
MX1	1	1	0	1
MYH11	1	1	1	1
NCAM1	1	1	1	1
NEUROD2	1	1	0	1
NFIC	1	1	0	1
NFIX	1	1	1	1
NGFR	1	1	0	1
NHS	1	1	1	1
OVOL1	1	1	1	1
P2RY2	1	1	1	1
PDE3A	1	1	1	1
PDK2	1	1	1	1
PDPK1	1	1	0	1
PECAM1	1	1	0	1
PEX10	1	1	1	1
POU2AF1	1	1	1	1
POU2F2	1	1	1	1
PPP1CB	1	1	1	1
PRLR	1	1	1	1

Gene	miRWalk	miRanda	RNA22	Targetscan
PRRG2	1	1	0	1
PSAP	1	1	0	1
PTBP1	1	1	1	1
RAB27B	1	1	0	1
RAD52	1	1	0	1
UPF1	1	1	0	1
RIT1	1	1	0	1
RNASEL	1	1	0	1
RPL22	1	1	0	1
RSU1	1	1	0	1
ATXN1	1	1	0	1
SH3BGRL	1	1	1	1
SHB	1	1	0	1
ST3GAL3	1	1	0	1
SIM1	1	1	1	1
SLC1A2	1	1	0	1
SLC6A1	1	1	1	1
SLC6A6	1	1	0	1
SLC6A12	1	1	0	1
SLC8A3	1	1	1	1
SMARCA4	1	1	0	1
SRMS	1	1	0	1
SRP19	1	1	0	1
SSX1	1	1	1	1
SSX2	1	1	1	1
SSX4	1	1	1	1
CDKL5	1	1	0	1
VAMP7	1	1	0	1
SYK	1	1	1	1
TECTB	1	1	0	1
TFDP2	1	1	1	1
TFRC	1	1	0	1
TNS1	1	1	1	1
TP53BP1	1	1	0	1
TP73	1	1	1	1
TPD52L2	1	1	1	1
TWIST1	1	1	0	1
CLIP2	1	1	1	1
WHSC1	1	1	0	1
MZF1	1	1	0	1
ZNF74	1	1	0	1
ZNF135	1	1	0	1
ZNF213	1	1	0	1
RAB7A	1	1	0	1
ALDH5A1	1	1	0	1
CUL3	1	1	0	1
CHST1	1	1	0	1
KLF7	1	1	1	1
KCNK5	1	1	0	1
SLC4A4	1	1	1	1
VAMP4	1	1	0	1
NRP2	1	1	1	1
SYNGAP1	1	1	0	1
CACNA2D2	1	1	0	1

Gene	miRWalk	miRanda	RNA22	Targetscan
MED20	1	1	0	1
H2AFY	1	1	0	1
PREPL	1	1	1	1
ABCG1	1	1	1	1
ZNF516	1	1	1	1
USP6NL	1	1	0	1
KIAA0141	1	1	0	1
ARHGEF17	1	1	0	1
TECPR2	1	1	0	1
IQSEC1	1	1	1	1
PAN2	1	1	0	1
YAF2	1	1	1	1
ALYREF	1	1	0	1
6-Mar	1	1	0	1
CACNG2	1	1	0	1
SEC24B	1	1	1	1
ENOX2	1	1	1	1
ATG7	1	1	1	1
CELF1	1	1	1	1
NFAT5	1	1	1	1
TRAF3IP2	1	1	1	1
NUP50	1	1	1	1
CPLX2	1	1	1	1
WDR6	1	1	1	1
PDZD2	1	1	0	1
MYT1L	1	1	1	1
NMNAT2	1	1	1	1
SIPA1L3	1	1	0	1
8-Sep	1	1	0	1
LARP4B	1	1	1	1
ATP11A	1	1	1	1
CAMTA1	1	1	0	1
CLEC16A	1	1	0	1
CLUH	1	1	1	1
MGRN1	1	1	0	1
WSCD1	1	1	1	1
SIN3B	1	1	0	1
KIAA0930	1	1	1	1
SLC9A8	1	1	1	1
SMG5	1	1	0	1
ICMT	1	1	0	1
PIK3R5	1	1	1	1
TNPO3	1	1	0	1
RBFOX2	1	1	1	1
ZNF324	1	1	0	1
RAB26	1	1	0	1
CNRIP1	1	1	0	1
SAMHD1	1	1	0	1
SIN3A	1	1	1	1
C2CD2	1	1	1	1
C16orf72	1	1	0	1
FTSJ2	1	1	1	1
TNPO2	1	1	0	1
EHD2	1	1	0	1

Gene	miRWalk	miRanda	RNA22	Targetscan
FOXP3	1	1	1	1
C3orf18	1	1	0	1
SLC25A37	1	1	0	1
CHST15	1	1	0	1
SCARA3	1	1	1	1
EVL	1	1	1	1
METTL13	1	1	0	1
GET4	1	1	1	1
RSF1	1	1	1	1
FGFRL1	1	1	1	1
KCNK10	1	1	0	1
SEMA5B	1	1	1	1
NEURL1B	1	1	1	1
DDX56	1	1	0	1
KLHDC4	1	1	0	1
TET2	1	1	1	1
BNC2	1	1	0	1
MBTD1	1	1	1	1
INO80D	1	1	1	1
GEMIN8	1	1	0	1
CCDC40	1	1	0	1
DALRD3	1	1	0	1
ARMC1	1	1	0	1
PPP1R9A	1	1	1	1
ZNF407	1	1	0	1
NSUN5	1	1	0	1
VAC14	1	1	1	1
LRRC8A	1	1	1	1
SLC2A9	1	1	0	1
SLC2A4RG	1	1	0	1
KCMF1	1	1	0	1
CCDC177	1	1	0	1
RGMA	1	1	0	1
ANO2	1	1	1	1
NAT14	1	1	0	1
KIAA1161	1	1	0	1
SEMA6A	1	1	1	1
PDZD4	1	1	1	1
GOLPH3	1	1	0	1
LMBR1	1	1	1	1
HIF3A	1	1	1	1
INF2	1	1	0	1
MRPS25	1	1	1	1
FUNDC2	1	1	0	1
OTUB2	1	1	0	1
ELOVL6	1	1	0	1
C1orf116	1	1	1	1
TMEM204	1	1	0	1
PPP1R3B	1	1	1	1
FBXO31	1	1	0	1
GGNBP2	1	1	0	1
CCDC68	1	1	0	1
GPR63	1	1	0	1
SLC38A1	1	1	0	1

Gene	miRWalk	miRanda	RNA22	Targetscan
SCRT1	1	1	0	1
ZMIZ2	1	1	1	1
OBSCN	1	1	1	1
DDI2	1	1	0	1
GPR123	1	1	1	1
DOT1L	1	1	0	1
MCM8	1	1	1	1
PLXDC2	1	1	0	1
MYOCD	1	1	1	1
ZNF618	1	1	0	1
WDFY2	1	1	0	1
ERP27	1	1	0	1
ANKS3	1	1	0	1
TBC1D16	1	1	0	1
GJD3	1	1	0	1
UBE2QL1	1	1	0	1
TOM1L2	1	1	0	1
MFSD4	1	1	0	1
PLEKHG4B	1	1	0	1
CLEC2L	1	1	0	1
ESCO2	1	1	0	1
TDRP	1	1	1	1
TTLL11	1	1	0	1
KIAA1958	1	1	1	1
ZFPM1	1	1	0	1
AGO4	1	1	1	1
APOBEC3F	1	1	0	1
SPRED2	1	1	0	1
ZNF449	1	1	0	1
AMER3	1	1	1	1
MPEG1	1	1	0	1
ZDHHC20	1	1	0	1
MDGA1	1	1	0	1
ZNF841	1	1	0	1
RNF212	1	1	0	1
SCARA5	1	1	1	1
KY	1	1	0	1
OR2A1	1	1	0	1
POLN	1	1	0	1
LHFPL4	1	1	0	1
ZNF805	1	1	0	1
SAMD12	1	1	0	1
SSX4B	1	1	1	1
FAM196A	1	1	0	1
ASAH2B	1	1	0	1
SSX2B	1	1	1	1
DNLZ	1	1	1	1
LOC100507747	1	1	0	1
LOC101928841	1	1	0	1
LOC101929479	1	1	0	1
LOC101929847	1	1	0	1

1 "1": Yes; "0":No.